JOURNAL OF Materials CHEMISTRY

Synthesis of nickel nanoparticles in aqueous cationic surfactant solutions

Dong-Hwang Chen* and Chih-Hsuan Hsieh

Department of Chemical Engineering, National Cheng Kung University, Tainan, Taiwan, 701, R.O.C.. E-mail: chendh@mail.ncku.edu.tw; Fax: 886-6-2344496; Tel: 886-6-2757575 (Ext. 62680)

Received 18th January 2002, Accepted 30th April 2002
First published as an Advance Article on the web 10th June 2002

The synthesis of nickel nanoparticles by the reduction of nickel chloride with hydrazine in an aqueous solution of cationic surfactants CTAB/$TC_{12}AB$ was studied. It was found that an appropriate amount of NaOH, trace acetone, and an elevated temperature were necessary for the formation of pure nickel nanoparticles. Also, it was not necessary to perform the reaction under a nitrogen atmosphere. X-ray diffraction revealed the resultant particles were pure nickel crystalline with a face-centered cubic (fcc) structure. Their mean diameter was 10–36 nm, increasing with increasing nickel chloride concentration or decreasing hydrazine concentration. When the concentration ratio of hydrazine to nickel chloride was above 40, the mean diameter approached a constant value. The magnetic measurement on a typical sample with a mean diameter of 12 nm showed that the resultant nickel nanoparticles were superparamagnetic due to their extremely small size. The saturation magnetization, remanent magnetization, and coercivity were 32 emu g^{-1}, 5.0 emu g^{-1}, and 40 Oe, respectively. Also, the magnetization was observed to increase with decreasing temperature. All the observed magnetic properties essentially reflected the nanoparticle's nature.

Introduction

In the past two decades, considerable attention has been devoted to the synthesis of metal nanoparticles because of their unusual properties and potential applications in optical, electronic, catalytic, magnetic materials, and so on.[1–7] A number of methods have been developed for the preparation of metal nanoparticles, such as photolytic reduction,[8] radiolytic reduction,[9] sonochemical method,[10] solvent extraction reduction,[11] microemulsion technique,[12] polyol process,[13] and alcohol reduction.[14]

Among the various kinds of metal nanoparticles, the preparation of some metal nanoparticles such as nickel, copper, and iron, are relatively difficult because they are easily oxidized. Nickel nanoparticles have attracted much attention because of their applications as catalysts and conducting and magnetic materials. Until now, only a few works on the preparation of nickel nanoparticles have been reported and they usually were performed in organic media to avoid the formation of nickel oxide or hydroxide.[13,15] The synthesis of pure Ni nanoparticles in aqueous solution without the formation of nickel oxides or hydroxides has not been achieved until now.

Aqueous surfactant systems have been used to produce some metal and semiconductor nanoparticles such as Au, Ag, CdS, and CdSe.[16–21] Their use in the synthesis of nickel nanoparticles has not been reported. In this work, the preparation of nickel nanoparticles in an aqueous solution of cationic surfactants CTAB/$TC_{12}AB$ was attempted. The particle size and structure of the resultant nanoparticles have been characterized by transmission electron microscopy (TEM) and X-ray diffraction (XRD). The effects of nickel chloride and hydrazine concentrations on particle sizes have been investigated and discussed. The magnetic properties of the nickel nanoparticles have also been examined by the superconducting quantum interference device (SQUID) magnetometer.

Experimental section

The cationic surfactant cetyltrimethylamonium bromide (CTAB) was obtained from Acros Organics (Belgium). The cationic co-surfactant tetradodecylammonium bromide ($TC_{12}AB$) and acetone were supplied by Aldrich (Milwaukee). Hydrazinium hydroxide was a guaranteed reagent of E. Merck (Darmstadt). Nickel chloride and sodium hydroxide were the products of Hayashi (Osaka). The water used throughout this work was reagent-grade water produced by a Milli-Q SP Ultra-Pure-Water Purification System of Nihon Millipore Ltd., Tokyo.

Typically, an aqueous solution of 10 mL was first prepared by dissolving CTAB (0.025 M), $TC_{12}AB$ (0.5 mg mL^{-1}) and nickel chloride (0.005–0.1 M) and trace acetone (10 μL mL^{-1}) in water. Then, hydrazine (0.05–1.25 M) and trace NaOH solution (1.0 M, 20 μL mL^{-1}) were added in sequence. At an elevated temperature of 60 °C, nickel nanoparticles were formed after about 1 h. The reduction reaction could be expressed as

$$2Ni^{2+} + N_2H_4 + 4OH^- \rightarrow 2Ni + N_2 + 4H_2O \quad (1)$$

The particle sizes were determined by TEM using a JEOL Model JEM-1200EX at 80 kV. The sample for TEM analysis was obtained by diluting the dispersed solution with ethanol and then placing a drop of the diluted solution onto a Formvar-covered copper grid and evaporating in air at room temperature. Before withdrawing the samples, the nickel-nanoparticle-dispersed ethanol solutions were sonicated for 1 min to obtain a better particle dispersion on the copper grid. XRD measurements were performed on a Rigaku D/max III. V X-ray diffractometer using Cu-Kα radiation ($\lambda = 0.1542$ nm). The magnetic measurements were done using the SQUID magnetometer (MPMS7, Quantum Design). The samples for XRD and magnetic analyses were obtained by recovering the

 DOI: 10.1039/b200603k

nickel nanoparticles from the solution using a permanent magnet, then washing the precipitates using ethanol, and finally vacuum drying at room temperature.

Results and discussion

According to some preliminary experiments, it was found that an elevated reaction temperature and the additions of trace acetone and NaOH solution were necessary for the formation of nickel nanoparticles in an aqueous solution of cationic surfactants CTAB/$TC_{12}AB$. Trace acetone (10 μL mL^{-1}) could be mixed with water and its content in the reaction medium was so low (<1wt.%), it was used for loosening the micellar framework.[17] An elevated reaction temperature this should be helpful for accelerating the formation rate of the nickel nanoparticles. It was found that the formation of the nickel nanoparticles was completed after 1 h at 60 °C, whereas no significant reaction occurred at 25 °C even after 24 h. The role of trace NaOH (1.0 M, 20 μL mL^{-1}) in the synthesis of the Ni nanoparticles is interesting. The addition of trace NaOH led to an increase of solution pH from 10.2 to 10.6. However, no nickel nanoparticles were formed if more hydrazine was added to raise the solution pH up to 10.6. This revealed that the trace NaOH did not play the simple role of adjusting the solution pH in the formation of the nickel nanoparticles. It suggested that the trace NaOH probably acted as a catalyst or a micellar structure modifier. Further investigation is necessary.

It is also notable that the preliminary experiments showed that no matter whether the synthesis reaction was performed in an inert atmosphere (N_2 gas), only metallic nickel nanoparticles were obtained. Phase analysis by XRD revealed that no oxides or hydroxide such as NiO, Ni_2O_3, and $Ni(OH)_2$ were formed. This could be attributed to the observed phenomenon that N_2 gas was produced and bubbled up continuously during the reaction as revealed by eqn. (1). So, it could be suggested that the N_2 gas produced might auto-create an inert atmosphere and hence the input of extra N_2 gas was not necessary for the synthesis of the nickel nanoparticles in this study.

A typical transmission electron micrograph and the size distributions for the nickel nanoparticles are shown in Fig. 1. The particles essentially were very fine and roughly monodispersed with a mean diameter of 12 nm. This reveals that the micelles composed of CTAB and $TC_{12}AB$ indeed restricted the growth of nickel nanoparticles efficiently. The corresponding XRD spectrum for the resultant particles is shown in Fig. 2. Three characteristic peaks for nickel (2θ = 44.5, 51.8 and 76.4), marked by their indices ((111), (200), and (222)) were observed. This also revealed that the resultant particles were pure fcc nickel. Accordingly, it could be concluded that the

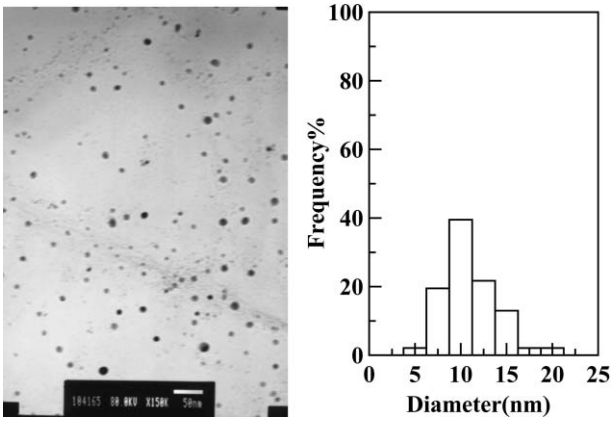

Fig. 1 Typical TEM micrograph and size distribution of nickel nanoparticles. [$NiCl_2$] = 0.025 M; [N_2H_5OH] = 1.0 M; [CTAB] = 0.025 M; [$TC_{12}AB$] = 0.5 mg mL^{-1}; 60 °C.

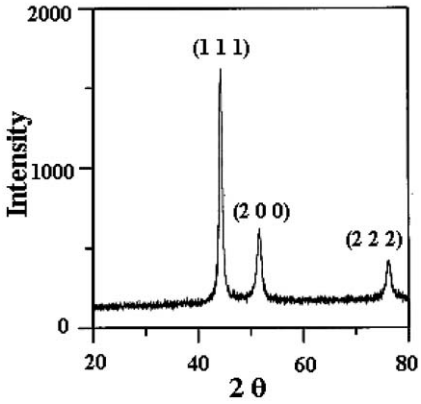

Fig. 2 X-ray diffraction spectrum of nickel nanoparticles. [$NiCl_2$] = 0.025 M; [N_2H_5OH] = 1.0 M; [CTAB] = 0.025 M; [$TC_{12}AB$] = 0.5 mg mL^{-1}; 60 °C.

nanoparticles prepared in this work were of pure nickel with fcc structure.

In addition, it was clear that the resultant nickel nanoparticles all were spherical, as indicated in Fig. 1. No rod-like or fiber-like particles were observed as reported in the cases of Au, CdS, and CdSe.[17–19,21] This could be attributed to the fact that the micelles were dynamic structures and the particle morphology was kinetically controlled. The addition of trace cyclohexane (10 μL mL^{-1}) to enhance the formation of the elongated rod-like micelle[17–18,22] was also attempted in this study. However, the XRD analysis showed the product was a mixture of Ni and $Ni(OH)_2$. The mechanism is not clear and needs further investigation, but it was definite that the addition of cyclohexane was not appropriate for the synthesis of nickel nanoparticles in the aqueous surfactant system used in this work.

The concentration effects of hydrazine and nickel chloride on the size of the nickel nanoparticles are shown in Figs. 3 and 4, respectively. At [$NiCl_2$] = 0.025 M, the mean diameters of the nickel nanoparticles decreased with increasing hydrazine concentration, and approached a constant value when the hydrazine concentration was above 1.0 M. At a constant

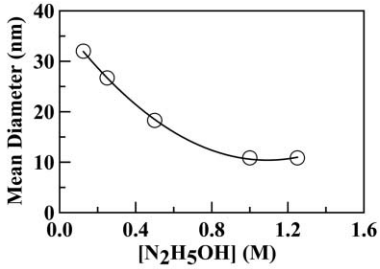

Fig. 3 Effect of hydrazine concentration on mean diameter of nickel nanoparticles. [$NiCl_2$] = 0.025 M; [CTAB] = 0.025 M; [$TC_{12}AB$] = 0.5 mg mL^{-1}; 60 °C.

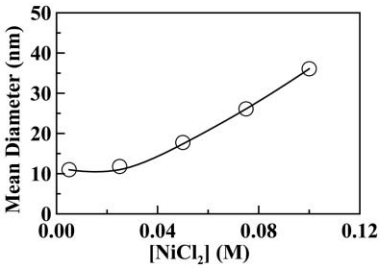

Fig. 4 Effect of nickel chloride concentration on mean diameter of nickel nanoparticles. [N_2H_5OH] = 1.0 M; [CTAB] = 0.025 M; [$TC_{12}AB$] = 0.5 mg mL^{-1}; 60 °C.

hydrazine concentration of 1.0 M, the mean diameters of the nickel nanoparticles increased with increasing nickel concentration and remained constant when $[NiCl_2] < 0.025$ M. Both effects were consistent with each other and revealed that the mean diameter of the nickel nanoparticles was not affected by either the hydrazine or nickel chloride concentrations when $[N_2H_5OH]/[NiCl_2] > 40$. This phenomenon could be explained from the influence of the reduction rate on the nucleation.

Since a minimum number of atoms was required to form a stable nucleus, a collision between several atoms must occur for nucleation. However, the probability was much lower than the probability for the collision between one atom and a nucleus already formed. That is, once the nuclei were formed, the growth process would be superior to nucleation. In addition, the resultant nanoparticles were roughly monodispersed. This might result from the fact that most nuclei were formed almost at the same time and grew at the same rate. Thus, the number of the nuclei formed at the very beginning of the reduction determined the number and size of the resultant particles. At a low hydrazine concentration, the reduction rate of nickel chloride was slow and only a few nuclei were formed during the early period of the reduction. The atoms formed during the later period were used mainly to collide with the nuclei already formed instead of forming new nuclei and this therefore led to the formation of larger particles. With an increase of hydrazine concentration, the enhanced reduction rate favored the generation of much more nuclei and the formation of smaller nickel nanoparticles. When the concentration ratio of hydrazine to nickel chloride was large enough, the reduction rate of nickel chloride was much faster than the nucleation rate and almost all the nickel ions were reduced to atoms before the formation of nuclei. The nucleation rate was not further raised and the number of nuclei held constant with increasing hydrazine concentration. Therefore, the size of the resultant nickel nanoparticles was not further reduced and was kept at a constant value.

Nickel is an important magnetic material. To further investigate the magnetic properties of the resultant nickel nanoparticles, a typical sample was taken for the magnetic measurement. The magnetization *versus* magnetic field plots (***M*–*H*** loops) at 25 °C are shown in Fig. 5. The quite weak hysteresis revealed the resultant nickel nanoparticles were nearly superparamagnetic. This could be attributed to the fact that the nickel nanoparticles were so small that they may be considered to have a single magnetic domain. From Fig. 5 and its enlargement near the origin (as shown in the inset), the saturation magnetization ($\boldsymbol{M}_s$), remanent magnetization ($\boldsymbol{M}_r$), and coercivity ($\boldsymbol{H}_c$) could be determined to be 32 emu g^{-1}, 5.0 emu g^{-1}, and 40 Oe, respectively.

The $\boldsymbol{M}_s$, $\boldsymbol{M}_r$, and $\boldsymbol{H}_c$ values of the bulk nickel at 300 K were about 55 emu g^{-1}, 2.7 emu g^{-1}, and 100 Oe, respectively.[23] The decrease in $\boldsymbol{M}_s$ might be due to the decrease in particle size and the accompanied increase in surface area. It is known that the energy of a magnetic particle in an external field is proportional to its size or volume *via* the number of magnetic molecules in a single magnetic domain. When this energy becomes comparable to the thermal energy, thermal fluctuations will significantly reduce the total magnetic moment at a given field.[24] In addition, the disorder structure in amorphous materials and at the interface, such as that found at a grain boundary, has been shown to cause a decrease in the effective magnetic moment.[23] Since the saturation magnetization of the nickel nanoparticles was reduced to 58% of the bulk nickel, the decrease in $\boldsymbol{M}_s$ of nickel nanoparticles also could be attributed to the presence of amorphous structure and the nonmagnetic or weakly magnetic interfaces. Furthermore, the magnetic molecules on the surface lack complete coordination and the spins are likewise disordered.[24] This phenomenon is more significant for nanoparticles due to their large surface-to-volume ratio and may be another factor that leads to the decrease in $\boldsymbol{M}_s$. Finally, the electron exchange between ligand and surface atoms could also quench the magnetic moment.[25] Although the nickel nanoparticles have been washed before the magnetic measurement, the very slight amount of the adsorbed surfactant molecules on the nickel nanoparticles also could cause a decrease in saturation magnetization. Accordingly, it is reasonable that the magnetization of nanoparticles is usually smaller than that of the corresponding bulk materials.

The $\boldsymbol{H}_c$ value of the nickel nanoparticles was quite small and lower than that of the bulk nickel, revealing that the resultant nickel nanoparticles were close to the superparamagnetic state. The $\boldsymbol{M}_r$ value of the nickel nanoparticles was slightly higher than that of the bulk nickel. This might result from the differences in their microstructure.

A typical temperature dependence of the magnetization for the nickel nanoparticles at an applied field of 10 kOe is shown in Fig. 6. It is obvious that the magnetization increased with decreasing temperature at 5–400 K. This could be reasonably considered as a result of the decrease in thermal energy.

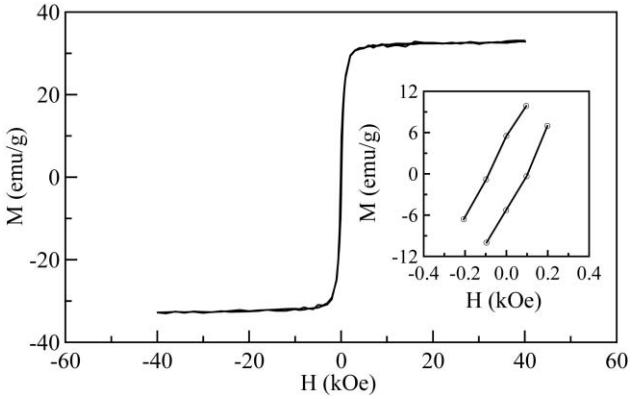

Fig. 5 Magnetization *versus* magnetic field for nickel nanoparticles at 25 °C. Mean diameter of nickel nanoparticles was 12 nm.

Conclusions

The synthesis of nickel nanoparticles has been achieved by a reduction of nickel chloride with hydrazine at 60 °C in an aqueous CTAB/TC_{12}AB solution containing trace acetone and NaOH. No extra nitrogen gas was required to create an inert atmosphere, and the resultant particles have been confirmed by XRD analysis as being pure nickel crystalline of fcc structure. The mean diameter of the nickel nanoparticles (10–36 nm) decreased with increasing hydrazine concentration or decreasing nickel chloride concentration, and approached a constant value when the concentration ratio of hydrazine to nickel chloride was above 40. The effects of the hydrazine and nickel chloride concentrations could be explained from the reduction, nucleation, and growth processes. This suggested that the mean diameter of the nickel nanoparticles was determined mainly by the number of nuclei formed at the very beginning of reduction.

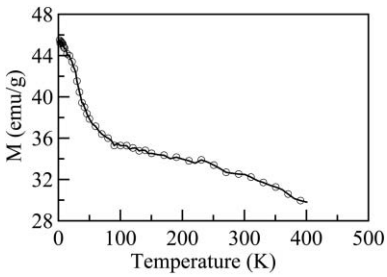

Fig. 6 Temperature dependence of the magnetization for nickel nanoparticles at an applied field of 10 kOe. Mean diameter of nickel nanoparticles was 12 nm.

Magnetic measurements indicated that nickel nanoparticles with a mean diameter of 12 nm had a saturation magnetization of 32 emu g^{-1}, a remanent magnetization of 5.0 emu g^{-1}, and a coercivity of 40 Oe at 25 °C, reflecting the nature of the nanoparticles. With a decrease of temperature in the range 5–400 K, the magnetization was also observed to increase because of the decrease in thermal energy.

This work is the first concerning the synthesis of Ni nanoparticles in an aqueous solution. The addition of trace acetone and NaOH are two key points for the preparation of pure Ni particles. Although the mechanism was not clear until now, undoubtedly, this work proposes an efficient and attractive method to produce pure Ni nanoparticles in aqueous media.

Acknowledgement

This work was performed under the auspices of the National Science Council of the Republic of China, under contract number NSC 90-2214-E006-009, to which the authors wish to express their thanks.

References

1 J. H. Fendler, *Chem. Rev.*, 1987, **87**, 877.
2 G. Schmid, *Chem. Rev.*, 1992, **92**, 1709.
3 P. V. Kamat, *Chem. Rev.*, 1993, **93**, 267.
4 L. N. Lewis, *Chem. Rev.*, 1993, **93**, 2693.
5 B. C. Gates, *Chem. Rev.*, 1995, **95**, 511.
6 L. L. Beecroft and C. K. Ober, *Chem. Mater.*, 1997, **9**, 1302.
7 N. Toshima and T. Yonezawa, *New J. Chem.*, 1998, 1179.
8 S. Remita, M. Mostafavi and M. O. Delcourt, *Radiat. Phys. Chem.*, 1996, **47**, 275.
9 J. H. Hodak, A. Henglein, M. Giersig and G. V. Hartland, *J. Phys. Chem. B*, 2000, **104**, 11708.
10 Y. Mizukoshi, K. Okitsu, Y. Maeda, T. A. Yamamoto, R. Oshima and Y. Nagata, *J. Phys. Chem. B*, 1997, **101**, 7033.
11 M. Brust, M. Walker, D. Bethell, D. J. Schiffrin and R. Whyman, *J. Chem. Soc., Chem. Commun.*, 1994, 801.
12 K. Osseo-Asare and F. J. Arriagada, *Ceram. Trans.*, 1990, **12**, 3.
13 L. K. Kurihara, G. M. Chow and P. E. Schoen, *Nanostruct. Mater.*, 1995, **5**, 607.
14 H. H. Huang, X. P. Ni, G. L. Loy, C. H. Chew, K. L. Tan, F. C. Loh, J. F. Deng and G. Q. Xu, *Langmuir*, 1996, **12**, 909.
15 D. H. Chen and S. H. Wu, *Chem. Mater.*, 2000, **12**, 1354.
16 T. Pal, T. K. Sau and N. R. Jana, *Langmuir*, 1997, **13**, 1481.
17 Y. Y. Yu, S. S. Chang, C. L. Lee and C. R. C. Wang, *J. Phys. Chem. B*, 1997, **101**, 6661.
18 C. C. Chen, C. Y. Chao and Z. H. Lang, *Chem. Mater.*, 2000, **12**, 1516.
19 N. R. Jana, L. Gearheart and C. J. Murphy, *Adv. Mater.*, 2001, **13**, 1389.
20 B. Nikoobakht and M. A. El-Sayed, *Langmuir*, 2001, **17**, 6368.
21 A. Kameo, A. Suzuki, K. Torigoe and K. Esumi, *J. Colloid Interface Sci.*, 2001, **241**, 289.
22 M. Törnblom and U. Henriksson, *J. Phys. Chem. B*, 1997, **101**, 6028.
23 J. H. Hwang, V. P. Dravid, M. H. Teng, J. J. Host, B. R. Elliott, D. L. Johnson and T. O. Mason, *J. Mater. Res.*, 1997, **12**, 1076.
24 K. V. P. M. Shafi, A. Gedanken, R. Prozorov and J. Balogh, *Chem. Mater.*, 1998, **10**, 3445.
25 D. A. van Leeuwen, L. M. van Ruitenbeek, L. J. de Jongh Ceriotti, G. Pacchioni, O. D. Häberlen and N. Rösch, *Phys. Rev. Lett.*, 1994, **73**, 1432.